Science in China Series E: Technological Sciences

A rapid forming method and simulation on controllable-porosity coating

ZHANG HaiOu†, HU BangYou & WANG GuiLan

School of Mechanical Science & Engineering, Huazhong University of Science and Technology, Wuhan 430074, China

A new method was introduced to fabricate porous coating and control its porosity by changing spray parameters. Two models were constructed to simulate the deformation of droplet and the deposition process of splats on substrate. Considering the gap-pore, step-pore and shield-pore in the presented models, the influence of spray angle on the porosity of coating was mainly investigated. The simulation and experimental results show that the presented method is suitable for fabricating controllable-porosity coating. The porosity of coating can reach 49%. When the spray angle is lower than 30°, the porosity of coating rapidly increases because of shielding effect. Moreover, powder size and impact velocity also influence the porosity. Besides, a new forming method of graded porous coating was simulated by continuously changing the spray angle.

plasma spray, porosity, spray angle, porous material, functional gradient material

Porous materials are widely used in modern industry fields such as fuel cell, biological tissue engineering, medicinal slow-release carrier, catalytic carrier, ceramic dust filter, water purifier, ceramic thermal insulating layer, and so on[1−8]. At present, the porous materials are mainly fabricated by powder casting and electrochemistry deposition. However, not only is the period long and the cost is high, but also it is difficult to control the porosity of coating through the above forming method. Plasma spray is suitable for rapidly forming coating for almost all kinds of materials. Many researches on plasma spray are devoted to increasing the density of coating by improving the spray technology or spray device. On the other hand, little attention has been devoted to the rapid forming of porous material and even gradual porous material. In principles, porous coating can be fabricated by controlling technical condition of plasma spray. Robot-based plasma spray is appropriate for fabricating the porous coating by controlling or changing the spray parameters. Based on plasma spray robot, we present a new method to fabricate the target porous material by controlling the parameters closely relate to porosity. Firstly, the growth models of coating are devel-

Received April 11, 2006; accepted March 19, 2007
doi: 10.1007/s11431-007-0061-x
†Corresponding author (email: zholab@hust.edu.cn)
Supported by the National Natural Science Foundation of China (Grant Nos. 50474053, 50475134)

oped to investigate the generation of pores in coating and the influence of spray parameters on porosity of coating. Then some experimental results are obtained to compare with the relevant simulation results. Finally, the fabrication method of graded porous coating is discussed by continuously changing plasma spray parameters related to the porosity of coating.

1 Theory

1.1 Deformation of droplet

In plasma spray, the molten degree of particle largely influences its deformation[9]. In the same impact condition, for example, semi-molten droplet would not flatten out entirely, and over-molten droplet would splash because of the rapid decrease on viscosity. According to the experimental observation, the shape of splat is approximately a thin cylinder when droplet impacts the substrate normally. If the spray angle, which indicates the closed angle between the axis of spray gun and the sprayed plane, is lower than 90°, the splat is approximately a shape of ellipsoid. Particles are melted and accelerated in plasma jet, impact substrate to form solid splats and deposit a coating on substrate. Regarding droplet as Newtonian, incompressible flow, its deformation on substrate obeys the conservation of mass and momentum[10,11]:

$$\nabla \cdot \boldsymbol{v} = 0, \tag{1}$$

$$\frac{\partial \boldsymbol{v}}{\partial t} + (\boldsymbol{v} \cdot \nabla)\boldsymbol{v} = \boldsymbol{f} - \frac{1}{\rho}\nabla p + \frac{\mu}{\rho}\nabla^2 \boldsymbol{v}, \tag{2}$$

where $\boldsymbol{v}$ is the velocity vector of mass point in the droplet, $\boldsymbol{f}$ the gravity, p the pressure, ρ the density and μ the viscosity of droplet.

The deformation of droplet also obeys the conservation of mechanical energy:

$$\frac{\mathrm{d}}{\mathrm{d}t}\left(E_k + E_p + L_f\right) = 0, \tag{3}$$

where E_k is kinetic energy, E_p potential energy of particles and L_f dissipation power of inner friction. While a droplet normally or obliquely impacts the substrate, the power flattening the droplet includes its kinetic energy gained from plasma flow and its gravitational potential energy. In fact, the gravitational potential energy is several orders less than the kinetic energy, so the gravitational potential energy is ignored in the simulation. According to the conclusions in ref. [12], the relation between Weber and Reynolds of droplet meets the following criterion:

$$We > 40.0(1-m)Re^{0.4}, \tag{4}$$

where m is wetting coefficient. The surface tension is ignored as the mechanical energy of droplet is consumed mainly by the viscosity resistance in the deformation process. Based on experimental measurement of splats, a fit model is built to evaluate the minor equatorial radius of splat b as follows:

$$b = \left(\frac{u^2 \sin^2 \alpha}{16200} + 1\right) r, \tag{5}$$

where r is the radius of the droplet, u impact velocity, and α spray angle. The splat is regarded as a cylinder when the droplet impacts the substrate normally. When the droplet obliquely impacts the substrate, it lengthens along its fly direction. According to the conservation of mechanical energy, the major equatorial radius of splat a is evaluated by the following equation:

$$a = b + \frac{\rho r^2 u \cos\alpha}{\mu}, \tag{6}$$

where ρ is the density of droplet and μ the viscosity. Suppose there is no splash in the deformation of droplet, the thickness of splat h is evaluated by the following equation according to the conservation of mass:

$$h = \frac{4r^3}{3ab}. \tag{7}$$

In real plasma spray, the viscosity of droplet is sensitive to its temperature. As the deformation time of droplet is extremely shorter than its solidification time, these two procedures are decoupled in simulation to simplify the evaluation. The deformation procedure of droplet is assumed to be an isothermal procedure. The viscosity of droplet in simulation is an equivalent value based on the assumption. The flattening ratio of splat ξ and its lengthening ratio ξ' are evaluated from the results of eqs. (5) and (6) as follows:

$$\xi = \frac{b}{r}, \tag{8}$$

$$\xi' = \frac{a}{b}. \tag{9}$$

1.2 Distribution of splat

During plasma spray, if spray gun is fixed to the substrate, droplet impacts the substrate and forms a circular area, which is called spray spot or particle footprint. When the spray gun is normal to the substrate, the distribution of splats in this spray spot approximately obeys Gaussian distribution as follows[13]:

$$p(x,y) = \frac{1}{2\pi\sigma}\exp\left(-\frac{x^2+y^2}{2\sigma^2}\right), \quad -\infty < x < +\infty, -\infty < y < +\infty. \tag{10}$$

Generating some random impact points based on this distribution function on computer, rotating and projecting it to the substrate again, a computational model is built to describe the splat distribution in spray spot when the spray gun is not normal to the substrate (Figure 1).

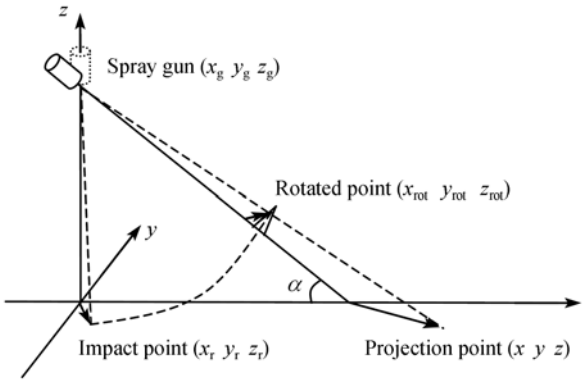

Figure 1 Computational model of splat distribution in spray spot with spray angle α.

Firstly, the random Gaussian coordinates of impact point of droplet in a unit circle area are calculated via

$$\begin{pmatrix} x_{\mathrm{r}} \\ y_{\mathrm{r}} \end{pmatrix} = \sqrt{\frac{-2\ln s}{s}} \begin{pmatrix} r_x \\ r_y \end{pmatrix}, \tag{11}$$

where r_x and r_y are random numbers within [−1,1] directly generated by computer, and $s = r_x^2 + r_y^2$ (s<1).

The spray plane is regarded as the *xoy* plane coordinates, and then the 3-D random coordinates of splat are expressed as follows:

$$\begin{pmatrix} x_v \\ y_v \\ z_v \end{pmatrix} = r_{\mathrm{s}} \begin{pmatrix} x_{\mathrm{r}} \\ y_{\mathrm{r}} \\ 0 \end{pmatrix} + \begin{pmatrix} x_{\mathrm{g}} \\ y_{\mathrm{g}} \\ 0 \end{pmatrix}, \tag{12}$$

where r_{s} is the radius of spray spot, $(x_{\mathrm{g}}\ y_{\mathrm{g}}\ 0)^{\mathrm{T}}$ the projection of the coordinates of spray gun $(x_{\mathrm{g}}\ y_{\mathrm{g}}\ z_{\mathrm{g}})^{\mathrm{T}}$ on the *xoy* plane. Turning the point $(x_{\mathrm{g}}\ y_{\mathrm{g}}\ z_{\mathrm{g}})^{\mathrm{T}}$ around the axis that is parallel with *y*-axis and passes through the spray gun point, the rotated coordinates of the point $(x_{\mathrm{rot}}\ y_{\mathrm{rot}}\ z_{\mathrm{rot}})^{\mathrm{T}}$ are given via the following equation:

$$\begin{pmatrix} x_{\mathrm{rot}} \\ y_{\mathrm{rot}} \\ z_{\mathrm{rot}} \end{pmatrix} = \begin{pmatrix} \sin\alpha & 0 & -\cos\alpha \\ 0 & 1 & 0 \\ \cos\alpha & 0 & \sin\alpha \end{pmatrix} \begin{pmatrix} x_v \\ y_v \\ z_v \end{pmatrix} + \begin{pmatrix} 1-\sin\alpha & 0 & \cos\alpha \\ 0 & 0 & 0 \\ -\cos\alpha & 0 & 1-\sin\alpha \end{pmatrix} \begin{pmatrix} x_{\mathrm{g}} \\ y_{\mathrm{g}} \\ z_{\mathrm{g}} \end{pmatrix}. \tag{13}$$

Projecting the rotated point to the substrate, the impacting point of droplet on the plane is calculated from the following equation:

$$\begin{pmatrix} x \\ y \\ z \end{pmatrix} = \begin{pmatrix} 1 & 0 & -l \\ 0 & 1 & -m \\ 0 & 0 & 0 \end{pmatrix} \begin{pmatrix} x_{\mathrm{rot}} \\ y_{\mathrm{rot}} \\ z_{\mathrm{rot}} \end{pmatrix}, \tag{14}$$

where $m = (x_{\mathrm{rot}} - x_{\mathrm{g}})/(z_{\mathrm{rot}} - z_{\mathrm{g}})$, $n = (y_{\mathrm{rot}} - y_{\mathrm{g}})/(z_{\mathrm{rot}} - z_{\mathrm{g}})$.

1.3 Splat quantity within unit length

On the basis of the Delesse's stereological principle, the porosity in a cross-section of a coating depicts the porosity of the coating. Considering the splats cut by a cross-section (Figure 2), a quasi-3D model based on the cross-section is constructed. Estimating the quantity of the splats deposited on the cross-section after the spray gun scans once over the substrate, the deposition process of splats is then rapidly simulated.

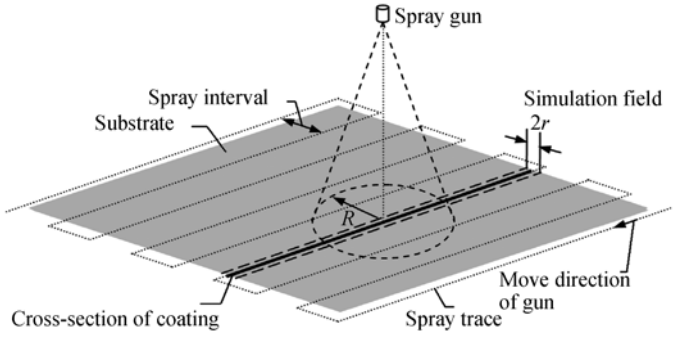

Figure 2 Plasma spray model using the zigzag scan path.

Shown in Figure 2 is the spray spot which is indicated by a circle when the spray gun is perpendicular to the substrate. After the spray gun scans over the sprayed surface once, the times of effectively scanning the cross-section is $S=1+2\times\lceil R/l\rceil$ (Figure 2). Taking a cross-section across the center of spray spot, the distance from the center of the splat that is cut by the cross-section to the cross-section is less than the radius of splat (Figure 3). Supposing $m=2\cdot\lceil R/l\rceil$, the quantity of deposited particles in the cross-section within unit length is evaluated from the following equation:

$$N=\frac{kF_0}{\overline{m}_{\mathrm{p}}v_{\mathrm{g}}}\sum_{i=-m}^{m}\int_{il-r}^{il+r}\int_{-\sqrt{R^2-y^2}}^{\sqrt{R^2-y^2}}p(x,y)\mathrm{d}x\mathrm{d}y, \tag{15}$$

where F_0 is powder feed, $\overline{m}_{\mathrm{p}}$ average mass of particles, v_{g} gun velocity, k deposition efficiency, l scan interval, R radius of spray spot, r radius of splat and $p(x, y)$ the Gaussian distribution function. This mathematic model is also suitable for the situation that the spray angle is lower than 90°. Using the model, the thickness of coating can be predicted indirectly. Moreover, this equation is also used for selecting the proper time step in simulation.

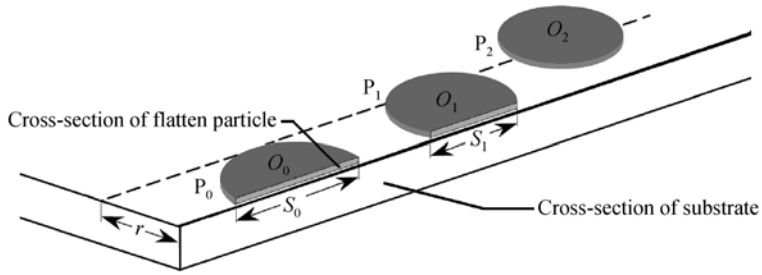

Figure 3 Computational model for the quantity of splats which are cut by cross-section. Splat P_0 and P_1 are counted rather than splat P_2 because P_2 is too far from the cross-section plane.

1.4 Deposition of splat

To simplify the numerical simulation process, some assumptions are used in the model: all particles are melted equably enough; diameter and position of particles obey Gaussian distribution; droplet impacts on the smooth substrate to form a splat of a thin cylinder shape[14−16]; the deformation of particle obeys mass conservation law, i.e. there is no splash in flattening process of droplet; splat spreads along the outline of the formed coating; both mass and thermal shock of the subsequent droplets are neglected. A pore is formed in the coating when the gap between two or more preceding splats is too narrow to fill or when the space is sheltered by the step at the edge of a preceding splat along the flying direction of droplet, which are respectively called gap-pore or step-pore. The size of gap relates to the material of particle and the condition of spray. At the edge of the current splat, the fluid of droplet spreads along its deformation direction without taking into account the gap or space under itself (Figure 4).

2 Experimental condition

The plasma spray device developed by HUST is used in experimental validation. Spray gun is installed at the end effector of Motoman UP20 robot to control the spray angle (Figure 5(a)). Ni-based substrates with the size of 20 mm × 20 mm × 30 mm are processed by the standard pro-

gram of rough grinding, fine grinding, polishing and cleaning to capture the flying particles. Before the plasma spray, the 45# steel plates with the size of 120 mm × 120 mm × 4 mm are ground, cleaned and heated up to 120℃. The spray path is set to be zigzag path, which is shown in Figure 5(b). The spray parameters are listed in Table 1.

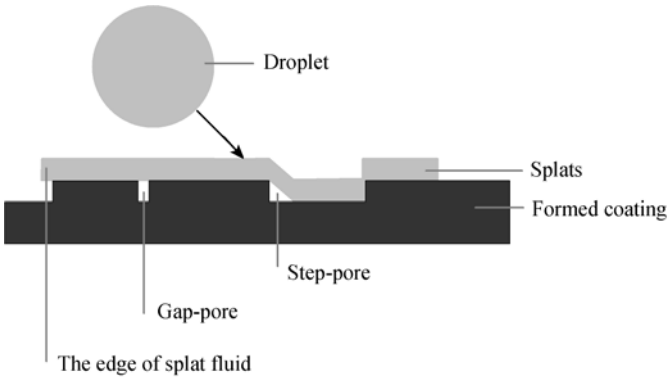

Figure 4 The sketch of deposition of splat and pore forming of coating.

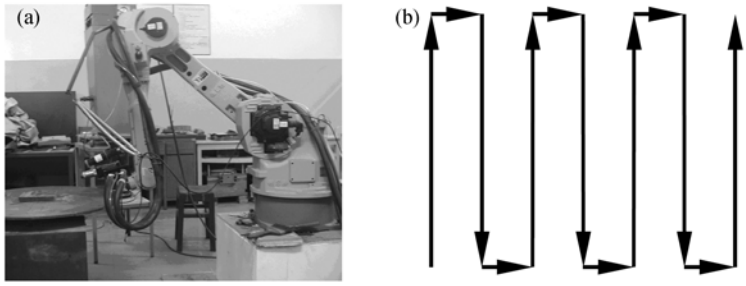

Figure 5 Gesture of spray gun in slantwise spray (a) and zigzag spray path (b).

Table 1 Technologic parameters of plasma spray

Type of powder	Size of powder	Powder feed	Power	Temperature of substrate	Spray distance	Gun velocity	Type of spray gun
45A Ni-based	70 μm	10 g/min	2000 W	120℃	120 mm	0.3 m/s	G781

3 Results and analysis

3.1 Influence of spray angle

3.1.1 Influence of spray angle on deformation and distribution of droplet. The SEM photos shown in Figure 6 indicate the deformation of molten particles on the substrate. Figure 6(a) shows the deformation with normal impacting. The splat is a thin cylinder with a few fingers. In Figure 6(b), a droplet hits the substrate with the spray angle of 30°. The splat clearly lengthens along the fly direction of droplet to form an approximate ellipsoid.

The splats distributions in spray spot are simulated at different spray angles in this paper (Figure 7). When the spray angle is less than 60° the outline of spray spot obviously presents a shape of ellipse rather than a circular area at normally spray. Decreasing the spray angle, splats tend to concentrate on the focus of ellipse that is near the spray gun. This trend is more and more obvious with the decrease of spray angle. These are consistent with the experimental results.

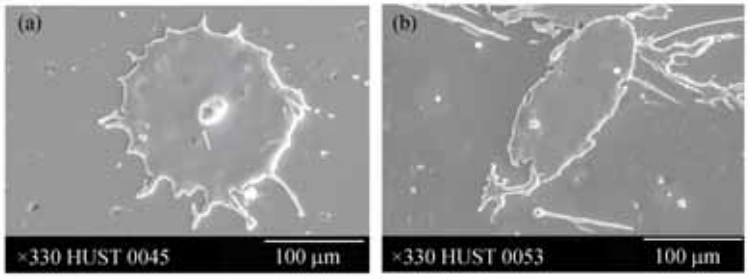

Figure 6 The SEM photos of splats with normal impact (a) and oblique impact (b).

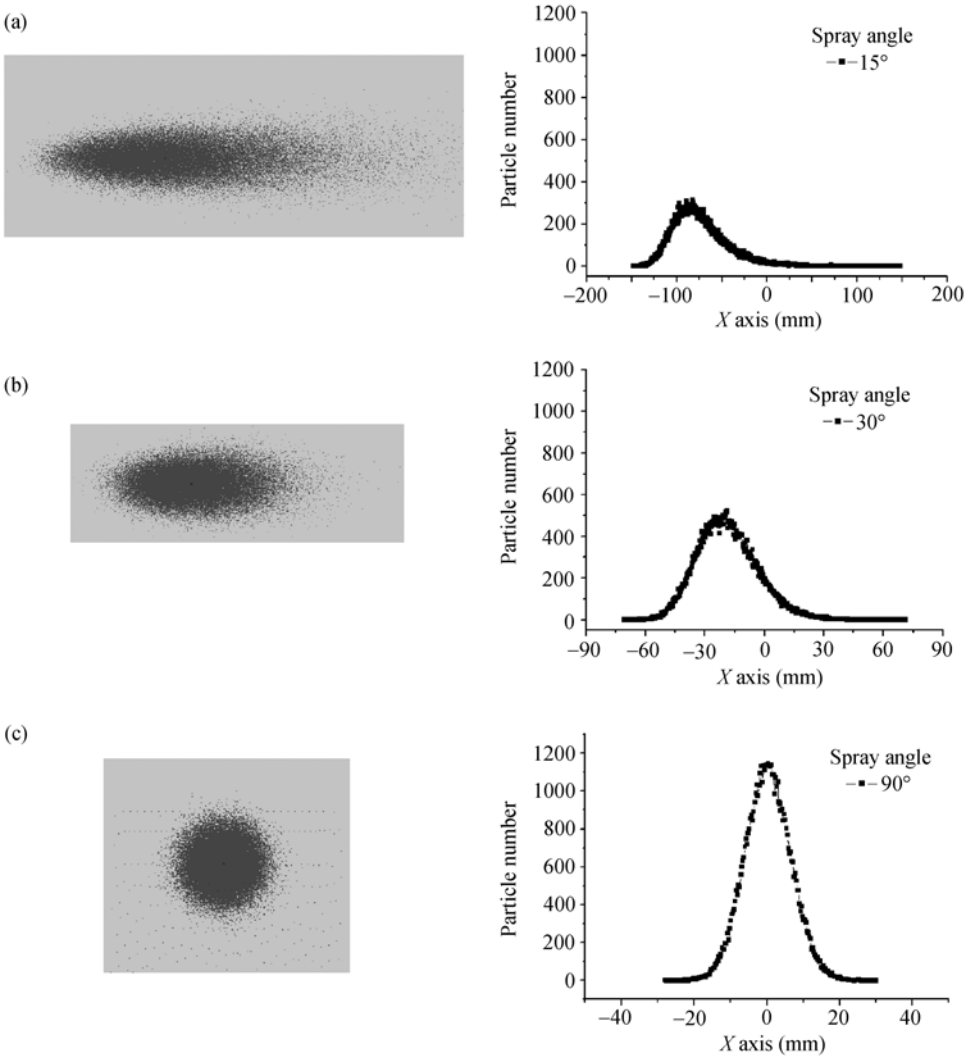

Figure 7 Splats distributions and distributional curves at the spray angles of 15° (a), 30° (b) and 90° (c).

3.1.2 Influence of spray angle on porosity of coating. Setting the spray angles at 15°, 30° and 90°, the coatings are respectively fabricated by plasma spray robot UP20. From the micrographs of cross-section with the amplification coefficient of 100 shown in Figure 8(a)—(c), shapes of pore in

coatings are quite different. Many through holes exist in the coating, as seen from Figure 8(a), and gradually disappear in Figure 8(b) and (c). The corresponding simulation results shown in Figure 8(d)—8(f) demonstrate the same characteristics. The simulation parameters are listed in Table 2.

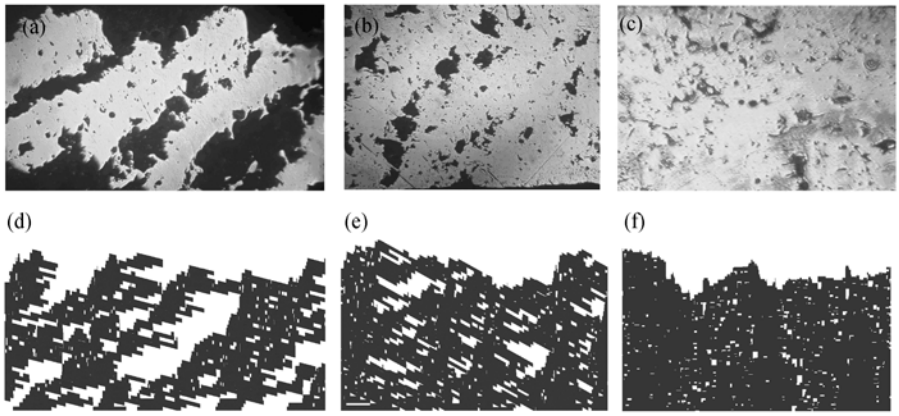

Figure 8 Experimental and simulated films at different spray angles. (a), (b) and (c) are experimental results at the spray angles of 15°, 30° and 90°, of which the porosities are 37.2%, 19.6% and 4.5%; (d), (e) and (f) are the respective simulation results, of which the porosities are 35.6%, 21.3% and 4.2%, respectively.

Table 2 Parameters in simulation

Diameter of particle	Particle velocity	Gun velocity	Powder feed	Gun distance	Radius of spray spot	Time step
70 μm	180 m/s	0.3 m/s	10 g/min	120 mm	20 mm	10^{-4} s

In simulation, the cross-section of size of 1 mm × 100 mm is divided into a grid of 1000×100000 elements. The size of element is 1 μm × 1 μm. Figure 8(d)—(f) are simulation cross-sections of coatings, of which the structures are different from each other. The porosity of coatings decreases with the increasing of spray angle, which is in accordance with the experimental micrographs. These results are closer experimental results than in ref. [15]. The curve shown in Figure 9 is about the influence of spray angle on porosity of coating. It is divided into three segments A_1, A_2 and A_3. Segment A_1 shows the little influence of spray angle on porosity when the spray angle is more than 60°, which indicates that the pores in film mainly consist of gap-pore in this part. The porosity of coating is very small and is influenced lightly by the spray angle. Therefore this segment is suitable for manufacturing compact coating. Segment A_2 shows that the porosity of coating obviously

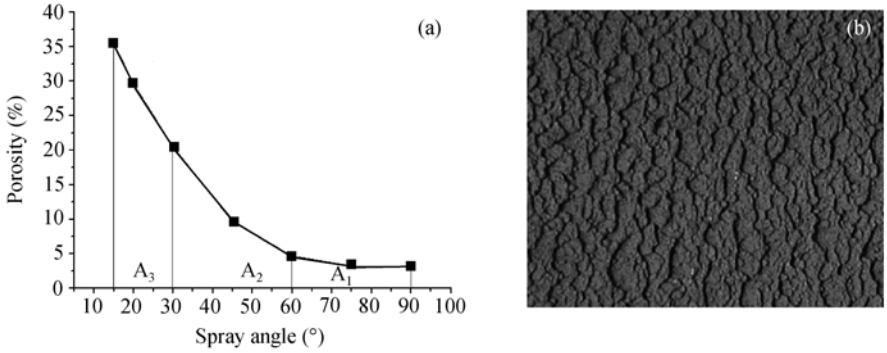

Figure 9 Porosity curve of simulation (a) and top appearance of coating with shielding pores (b).

increases when the spray angle decreases, which indicates the obvious influence of step effect on the porosity of coating.

It is seen from segment A_3 that the porosity of coating rapidly increases with the decreasing of spray angle. When the spray angle is very small (<30°) droplets comparatively concentrate on the focus of spray spot near the spray gun. This situation causes the shielding effect among splats. Thus, many pores called shield-pore are formed in the coating. The shield-pore has nothing to do with the height of step of single splat. It is gradually formed via affixing one splat to another. Therefore the diameter of shield-pore, which is about 100 μm, is greatly larger than the gap-pore. There are many through holes in the real plasma spray coating, which demonstrates the related simulation results are effective.

3.2 Influence of other spray parameters on porosity of coating

3.2.1 Scan velocity of spray gun. By changing different parameters such as gun velocity, particle size and droplet velocity, some simulation results are obtained on computer. The results shown in Figure 10(a) indicate that porosity of coating is increased with the decrease of the spray angle. But the influence of the scan velocity of spray gun on porosity of coating is not obvious. Commonly, the droplet velocity is greatly higher than the gun scan velocity, so the impacting behaviour of droplet is hardly influenced by the scan velocity of spray gun.

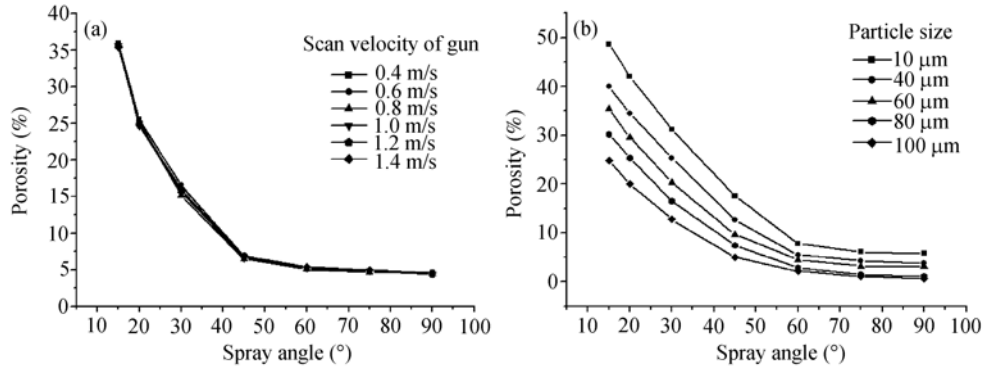

Figure 10 Influence of scan velocity of spray gun (a) and particle size on porosity of coating (b).

3.2.2 Particle size. The curves in Figure 10(b) show the influence of particle size on porosity at different spray angles. It is statistically obvious that the bigger the size of particle, the fewer the flat particles in same space. Therefore it is concluded that the porosity decreases with the increase of the particle size.

3.2.3 Impact velocity of droplet. Figure 11(a) shows that the porosity of coating decreases with the increase of droplet velocity. The increase of droplet velocity is favourable for the spread of droplet, so the heights of small gap and step are decreased. But when the spray angle is almost vertical or horizontal, the velocity of droplet scarcely influences the porosity of coating. When the spray angle is close to 90°, almost all the pores are gap-pores. For all droplets flat enough, the thickness of splat at different velocities is narrowly different, so the porosities are close to each other. On the other hand, when the spray angle is very small, all the pores nearly consist of shield-pores, whose size hardly relates to the thickness of single splat. Therefore the porosity of coating is not much different at the different droplet velocities either. In this case, gap-pore is a little part of all pores in coating and therefore could even be ignored numerically (Figure 11(b)).

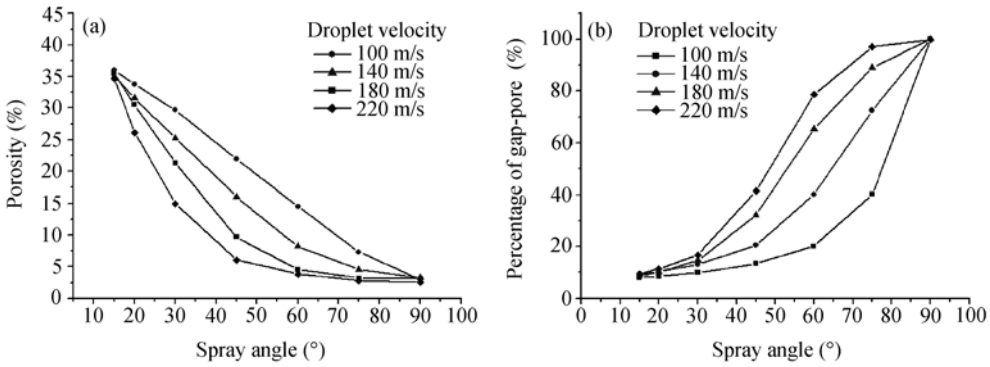

Figure 11 Influence of particle velocity on porosity of coating (a) and percentage of gap-pore to total porosity (b).

3.3 Simulation of forming graded porous coating

During the plasma spray process, the porous coating with variable porosity can be fabricated by continuously changing the spray angle. The simulation result of cross-section on graded porous coating is shown in Figure 12. It is seen that porosity of coating varies obviously along the vertical direction. The results shown in Figure 12(a) and (b) are under the conditions of increasing the spray angle from 15° to 90° linearly and non-linearly (Figure 12(c)). The porosity of the latter (26.5%) is larger than the former (18.39%). In Figure 12(b), the average porosity of coating is 26.5%, but the porosity of its underside part achieves 42.4%. It is a convenient method to rapidly manufacture the graded porous coating based on the robot.

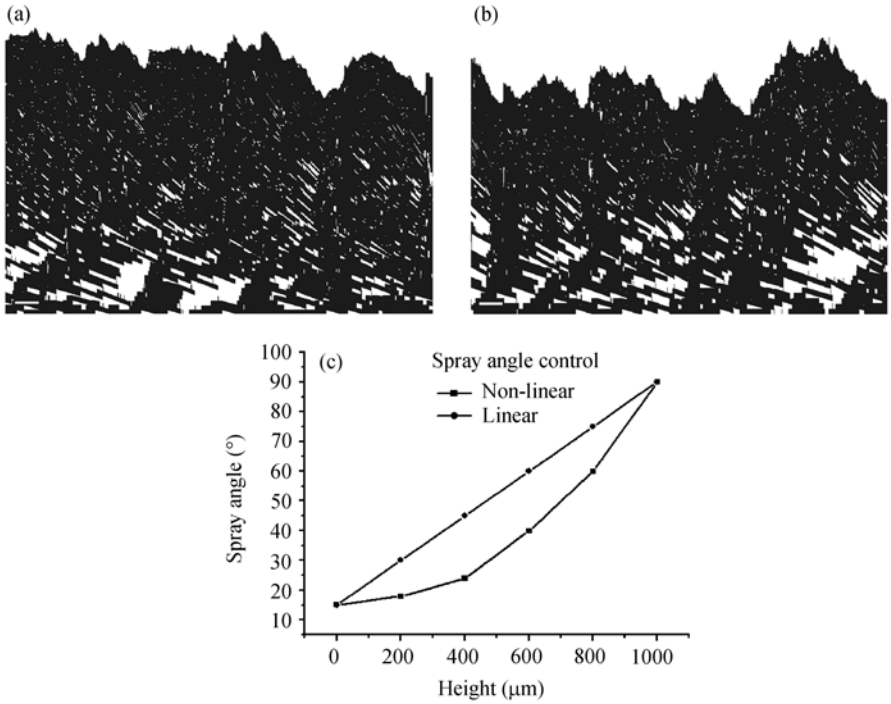

Figure 12 Cross-sections of graded porous coating with linear (a) and non-linear (b) variations on spray angle, of which the control curves are shown in (c).

4 Conclusions

(i) In this paper, a new method for rapidly forming the porous coating by changing spray angle is presented. By this method the controllable-porosity coating are fabricated. According to the related simulation results, our models that are constructed to simulate the deformation of droplet and the deposition of splats on substrate are effective.

(ii) The results show that the porosity of coating increases with the decrease of spray angle: when the spray angle is greater than 60° the variation of porosity is not obvious; when the spray angle is lower than 60° the porosity of coating begins to increase distinctly; especially when the angle is lower than 30° the porosity increases rapidly with the decrease of spray angle because of shielding effect.

(iii) When the spray angle is a constant, the porosity of coating decreases with the increase of the impact velocity and the size of droplet; but it is not obviously influenced by the scan velocity of spray gun.

(iv) Porosity of the coating gradually varies with the continuous change of the spray angle. It is realistically possible to rapidly fabricate graded porous materials.

1 Chen Y X, Wang G L, Zhang H O. Numerical simulation of coating growth and pore formation in rapid plasma tooling. Thin Solid Films, 2001, 390(1): 13—19

2 Wan G L, Wang W, Zhang H O, et al. Development on the performance of films on the interconnect of SOFC by plasma spray. Funct Mater (in Chinese), 2003, 2: 173—175

3 Markenscoff P, Zygowakis K. Pore structure and hydration rates modulate the release of bioactive agents from degradable scaffolds. In: Blanchard S M, Eckstein E C, Eds. Proceedings of The First Joint BMES/EMBS Conference Serving Humanity, Advancing Technology. Atlanta: IEEE Inc, 1999. 720—725

4 Stewart S, Ahmed R, Itsukaichi T. Contact fatigue failure evaluation of post-treated WC-NiCrBSi functionally graded thermal spray coatings. Wear, 2004, 257(9-10): 962—983

5 Wan Y P, Sampath S, Prasad V, et al. An advanced model for plasma spraying of functionally graded materials. J Mater Process Tech, 2003, 137(1-3): 110—116

6 Yoshikawa H, Myoui A. Bone tissue engineering with porous hydroxyapatite ceramics. J Artif Organs, 2005, 8: 131—136

7 Cetinel H, Uyulgan B, Tekmen C, et al. Wear properties of functionally gradient layers on stainless steel substrates for high temperature applications. Surf Coat Tech, 2003, 174-175: 1089—1094

8 Yu G, Nakamura T, Prchlik L, et al. Micro-indentation and inverse analysis to characterize elastic-plastic graded materials. Mater Sci Eng A, 2003, 345(1-2): 223—233

9 Chang C H, Pfender E. Advance in the computational modeling of thermal plasma processing. JOM, 1996, 48(6): 46—48

10 Delplanque J P, Rangel R H. A comparison of models, numerical simulation, and experimental results in droplet deposition process. Acta Metall Mater, 1998, 46(14): 4925—4933

11 Bertagnolli M, Marehese M, Jacucci G. Modeling of particles impacting on a rigid substrate under plasma spraying conditions. J Therm Spray Tech, 1995, 4(1): 41—49

12 Zhang H. Theoretical analysis of spreading and solidification of molten droplet during thermal spray deposition. Int J Heat Mass Transf, 1999, 42: 2499—2508

13 Marsaglia G, Narasimhan B, Zaman B, et al. A random number generator for PC's. Comput Phys Commun, 1990, 60(3): 345—349

14 Madejski J. Solidification of droplet on a cold face. Int J Heat Mass Transf, 1976, 19(9): 1009—1013

15 Yang Y -S, Kim H -Y, Chun J -H. Spreading and solidification of a molten microdrop in the molder jet bumping process. Compon Packag Tech, 2003, 26(1): 215—221

16 Zagorski A V, Stadelmaier F. Full-scale modelling of a thermal spray process. Surf Coat Tech, 2001, 146-147: 162—167